Development of high spatial resolution annual emission inventory of greenhouse gases from open straw burning in Northeast China from 2001 to 2020

Zihan Song[a,b], Leiming Zhang[c], Chongguo Tian[d], Qiang Fu[a,b], Zhenxing Shen[e],

Renjian Zhang[f], Dong Liu[a,b], Song Cui[a,b*]

[a] *International Joint Research Center for Persistent Toxic Substances (IJRC-PTS), School of Water Conservancy and Civil Engineering, Northeast Agricultural University, Harbin, Heilongjiang, 150030, China*

[b] *Research Center for Eco-Environment Protection of Songhua River Basin, Northeast Agricultural University, Harbin, Heilongjiang, 150030, China*

[c] *Air Quality Research Division, Science and Technology Branch, Environment and Climate Change Canada, Toronto, Ontario, M3H 5T4, Canada*

[d] *CAS Key Laboratory of Coastal Environmental Processes and Ecological Remediation, Yantai Institute of Coastal Zone Research, Chinese Academy of Sciences, Shandong Key Laboratory of Coastal Environmental Processes, YICCAS, Yantai, 264003, China*

[e] *Department of Environmental Sciences and Engineering, Xi'an Jiaotong University, Xi'an, 710049, China*

[f] *Institute of Atmospheric Physics, Chinese Academy of Sciences, Beijing 100029, China*

*Corresponding author: Dr. Song Cui   Email: cuisong-bq@neau.edu.cn (S. Cui)

WORD COUNT: 6000

7 FIGURES

1 TABLE

Abstract

Open straw burning has been widely recognized as a significant source of greenhouse gases (GHGs), posing critical risks to atmospheric integrity and potentially exacerbating global warming. In this study, we proposed a novel method that integrates crop cycle information into extraction and classification of fire spots from open straw burning in Northeast China from 2001 to 2020. By synergizing the extracted fire spots with the modified Fire Radiative Power (FRP) algorithm, we developed high spatial resolution emission inventories of GHGs, including carbon dioxide (CO_2), methane (CH_4), and nitrous oxide (N_2O). Results showed that the northern Sanjiang Plain, eastern Songnen Plain, and eastern Liao River Plain were areas with high intensity of open straw burning. The number of fire spots was evaluated during 2013-2017, accounting for 58.2% of the total fire spots observed during 2001-2020. The prevalent season for open straw burning shifted from autumn (pre-2016) to spring (post-2016), accompanied by a more dispersed pattern in burning dates. The two-decade cumulative emissions of CO_2, CH_4, and N_2O were quantified at 198 Tg, 557 Gg, and 15.7 Gg, respectively, amounting to 218 Tg of CO_2-eq. Significant correlations were identified between GHGs emissions and both straw yields and straw utilization ($p < 0.01$). The enforcement of straw burning bans since 2018 has played a pivotal role in curbing open straw burning, and reduced fire spots by 51.7% on annual basis compared to 2013-2017. The novel method proposed in this study considerably enhanced the accuracy in characterizing spatiotemporal distributions of fire spots from open straw burning and

47   quantifying associated pollutants emissions.

48   **Keywords:** Open straw burning; Fire spot; Crop cycle; Greenhouse gas; Emission

49   inventory

50   **Keywords Plus:** Open straw burning; MODIS; Fire spot; Accurate extraction; Crop

51   cycle; Crop type; Phenology; Greenhouse gas; Emission inventory; Driving factor;

52   Policy

59

1 Introduction

Open straw burning, a customary practice in agricultural areas, serves multiple purposes, including rapid straw disposal, weed control, nutrient release, and pest management (Korontzi et al., 2006; Wen et al., 2020). This practice results in short-term yet intense emissions of greenhouse gases (GHGs), such as carbon dioxide (CO_2), methane (CH_4), and nitrous oxide (N_2O). The accumulation of these gases in the atmosphere adversely impacts climate and atmospheric chemistry (Weldemichael and Assefa, 2016; Tang et al., 2020; Hong et al., 2023). To date, open straw burning remains prevalent in grain-producing areas globally, despite the many drawbacks of such a practice (Gadde et al., 2009; Huang et al., 2013; Zhu et al., 2015; Ahmed et al., 2019; Mehmood et al., 2020; Fu et al., 2022; Huang et al.,2023; Xu et al., 2023a). Thus, accurate and high spatial resolution emission inventories for GHGs from this source sector are needed from regional to global scales to assess potential climate and air quality impacts and formulate carbon mitigation policies.

The "bottom-up" approach, which is based on the amount of straw burned and corresponding emission factors, has been widely employed to establish emission inventories for various pollutants emitted from open straw burning (van der Werf et al., 2017; Wang et al., 2018; Liu et al., 2021; Zheng et al., 2023). Emission factors for diverse pollutants released from different types of straw burning have been extensively investigated in laboratory studies (Li et al., 2007; Liu et al., 2011; Stockwell et al., 2014;

81   Pan et al., 2017; Peng et al., 2016; Sun et al., 2016). However, estimation of the amount

82   of straw burned is subject to large uncertainties since it involves many parameters, such

83   as grain yield, ratio of straw and grain, open burning proportion, burning efficiency,

84   and dry matter fraction (Guan et al., 2017; Zhou et al., 2017). Consequently, existing

85   regional-scale emission inventories based on the "bottom-up" approach generally have

86   large uncertainties and low spatiotemporal resolutions (Tian et al., 2011; Jin et al., 2017).

87

88   The advent of satellite technologies, such as Moderate Resolution Imaging

89   Spectroradiometer (MODIS, remote sensing instrument), Visible Infrared Imaging

90   Radiometer Suite (VIIRS, remote sensing instrument), and Himawari-8 (geostationary

91   satellite), has markedly revolutionized the monitoring of open straw burning, enabling

92   real-time and high spatiotemporal resolution fire spot products to be accessible to the

93   general public (Schroeder et al., 2014; Giglio et al., 2016; Xu et al., 2017; Wu et al.,

94   2018; Zhuang et al., 2018; Lv et al., 2024). Many studies have effectively utilized

95   satellite fire spot products for constructing emission inventories, based on either the

96   burned area (BA) or fire spot counts (FC) (Ke et al., 2019; Cui et al., 2021). Several

97   studies have also developed a hybrid inventory strategy using the "bottom-up"

98   approach to allocate GHGs emissions spatially and temporally based on BA or FC (Jin

99   et al., 2018; Zhang et al., 2019; Kumar et al., 2021). These approaches have

100   significantly improved the spatiotemporal resolutions of the emission inventories for

101   open straw burning (Wu et al., 2023).

102

103 MODIS and VIIRS, both operating in polar orbits, provide only two observations per

104 day. MODIS has provided 1 km resolution fire data since 2000, which is suitable for

105 long-term trend analyses (Chen et al., 2012); while VIIRS has provided fire data at a

106 375 m resolution since 2012, which is more suitable for detecting small fires (Chen et

107 al., 2022). Himawari-8 (Geostationary orbit) has provided 10-minute temporal

108 resolution and 2 km spatial resolution fire data since 2015, ideal for real-time

109 monitoring across the Asia-Pacific region (Zhang et al., 2020). However, the

110 aforementioned datasets remain inadequate for accurately capturing small-area, short-

111 duration open straw burning, particularly in scattered farmlands (Wiedinmyer et al.,

112 2014). It should also be noted that meteorological disturbances, such as cloud cover and

113 rainfall, can reduce the accuracy of these products (Schroeder et al., 2014; Ying et al.,

114 2019). Furthermore, straw burning during non-satellite transit periods, on cloudy days,

115 at night, and under heavy haze may not be captured in these datasets (Liu et al., 2020).

116 For example, Liu et al. (2019) found that same-day omission error of MODIS burned

117 area product could be as high as 95% for agricultural fire detection during the post-

118 monsoon season in northwestern India.

119

120 With continuous enrichment of satellite data, a strong relationship was observed

121 between fire radiative power (FRP) and emission amounts from open straw burning

122 (Wu et al., 2023). Consequently, the FRP algorithm has been widely accepted for

123   estimating emissions (Wooster et al., 2005; Freeborn et al., 2008; Vermote et al., 2009;

124   Yang et al., 2019). The FRP algorithm has been optimized by integrating multi-source

125   satellite fire spot data, field survey data, and ground observation data, and combined

126   with advanced modeling techniques to improve the accuracy of emission inventory for

127   open straw burning. For example, Liu et al. (2020) revised FRP by combining

128   household survey results with satellite observations in northern India to capture small

129   fires, fill cloud/haze gaps in satellite observations, and adjust partial-field burns and

130   diurnal cycle of fire activity disturbances. Yang et al. (2020) improved the FRP

131   algorithm by calibrating the contributions of open straw burning to ground observation

132   data in Northeast China based on model simulation results using the coupled Weather

133   Research and Forecasting model and Community Multiscale Air Quality (WRF-CMAQ)

134   model.

135

136   At present, the identification of straw types in open straw burning typically relies on

137   crop data, such as the International Geosphere-Biosphere Programme (IGBP)-Modified

138   MODIS Land Use and MapSPAM datasets (Ke et al. 2019; Yang et al. 2020). These

139   low spatiotemporal resolution crop data contribute to errors in both the extraction of

140   fire spots and the identification of straw types (Ke et al., 2019; Liu et al., 2022).

141   Additional errors come from planting structure adjustment and frequent variations in

142   crop phenology. For instance, fire spots occurred during crop growth might be

143   incorrectly classified as open straw burning, while those occurred prior to crop growth

144 could be inaccurately attributed to burning of straws from subsequent harvests (Zhou

145 et al., 2022). Therefore, high spatiotemporal resolution data on crop types and

146 phenology are critical, and such data should be integrated into the extraction and

147 classification of fire spots from open straw burning to accurately estimate emissions of

148 various pollutants from this source sector.

149

150 To control emissions from open straw burning, the "Air Pollution Prevention and

151 Control Action Plan" (APPCAP) took into effect in 2013 in China (Huang et al., 2021).

152 In addition, China committed to achieve carbon peak by 2030 and carbon neutrality by

153 2060, which draws unprecedented challenges in reducing carbon emissions from open

154 straw burning (Wu et al., 2023). As a significant grain-producing region in China,

155 Northeast China produced 135 million tons of major grains (corn, rice, beans, and wheat)

156 in 2020, accounting for 21.4% of total production in China (National Bureau of

157 Statistics of China, 2021). During 2013-2018, open straw burning in Northeast China

158 exhibited an increasing trend, while decreasing in all other regions of China (Huang et

159 al., 2021). The constant increase reflects the expansion of the agricultural sector and

160 economic development in Northeast China yet relatively unconstrained open burning

161 activities (Huang et al., 2021). Liu et al. (2022) estimated CO_2 emissions from open

162 straw burning in Northeast China to be as high as 344 Tg from 2012 to 2020.

163

164 In this study, high spatial resolution fire spot products were used to develop annual

165   emission inventories of GHGs, including CO_2, CH_4, and N_2O, from open straw burning

166   in Northeast China for the period of 2001-2020. To improve the accuracy of the

167   developed emission inventory, a novel concept that integrates the crop cycle

168   information into fire spot extraction and classification was adopted. Furthermore, this

169   study conducted a thorough analysis to assess the driving factors influencing GHGs

170   emissions during the two decades. This study comprehensively examined GHGs

171   emissions from open straw burning in Northeast China and offered valuable insights to

172   policy makers for mitigating carbon emissions and air pollution in agricultural areas.

173   **2   Methodology**

174   **2.1 Extraction and classification of fire spots**

175   The MODIS fire product (MCD14ML, Collection 6.1) was selected from 1 January

176   2001 to 31 December 2020 for the whole region of Northeast China (Giglio et al., 2016,

177   sftp://fuoco.geog.umd.edu). The dataset, with a spatial resolution of about 1 km^2,

178   includes essential variables, such as latitude, longitude, acquisition date and time (in

179   UTC), satellite (Aqua or Terra), FRP, and fire type (presumably vegetation fire, active

180   volcano, other static land source, and offshore), among others (https://modis-

181   fire.umd.edu/files/MODIS_C6_C6.1_Fire_User_Guide_1.0.pdf). Non-vegetation fire

182   activities (active volcano, other static land source, and offshore) were then filtered out

183   from the selected dataset for subsequent analysis.

184

185   To clarify, the MCD14ML underestimated fire spots in 2001 and 2002 because only the

186   Terra satellite was operational before 3 July 2002. Therefore, data for the years of 2003

187   to 2020 were used for developing annual emission inventories, with relevant results for

188   2001 and 2002 as reference only. Also, a failure of the Aqua satellite on 16 August 2020

189   led to the loss of fire spot data for about two weeks (https://modis-

190   fire.umd.edu/files/MODIS_C61_BA_User_Guide_1.1.pdf). However, as August is a

191   crop-growing period in Northeast China, this failure would not lead to an

192   underestimation of fire spots from open straw burning.

193

194   The ChinaCropArea1 km and ChinaCropPhen1 km datasets were used to extract and

195   classify fire spots from open straw burning (Luo et al., 2020a; Luo et al., 2020b). These

196   datasets present annual data on the type and phenology (Day of Year (Doy) of

197   emergence and maturity) of grain crops (corn, rice, and wheat). Considering that

198   Northeast China is a major bean-producing area, we also compiled bean distribution

199   datasets (Li et al., 2021; Xuan et al., 2023). However, bean distribution in Jilin and

200   Liaoning provinces was not recorded during 2001-2012 in this dataset. The dataset was

201   extended to the whole region of Northeast China (Heilongjiang, Jilin, and Liaoning

202   provinces) after 2013. Thus, some gaps still exist in these datasets compared to the

203   comprehensive information required for this study, as detailed in **Table S1**.

204

205   **Fig. 1** describes the meticulous process to accurately extract and classify fire spots from

open straw burning in areas experiencing one-harvest season every year. The process

involves several key steps:

Step 1) The current year's ChinaCropPhen1 km and ChinaCropArea1 km, along with

the previous year's ChinaCropArea1 km data, were extracted to Fire spots (MCD14ML)

by ArcGIS 10.2 software to obtain the Fire spots-Crop-Phen dataset.

Step 2) Considering the crop cycle, the extraction of fire spots was divided into two

stages. The first stage is before crop growth (spring) and requires the fire spot to satisfy

two conditions: a) there was a crop planted in the previous year, and b) the burning date

is before emergence. The second stage is after crop growth (autumn) and also involves

two conditions: a) there was a crop planted in the current year, and b) the burning date

is after maturity.

Step 3) For fire spots in spring, the type of straw burned is identified based on the

previous year's crop type. For autumn fire spots, the straw type is determined according

to the crop type of the current year.

Furthermore, fire spots from open straw burning were extracted using the traditional

method that does not integrate crop cycle information. Only the current year's

ChinaCropArea1 km data was extracted to Fire spots (MCD14ML). Then, fire spots

occurring on agricultural land with growing crops were identified as open straw burning.
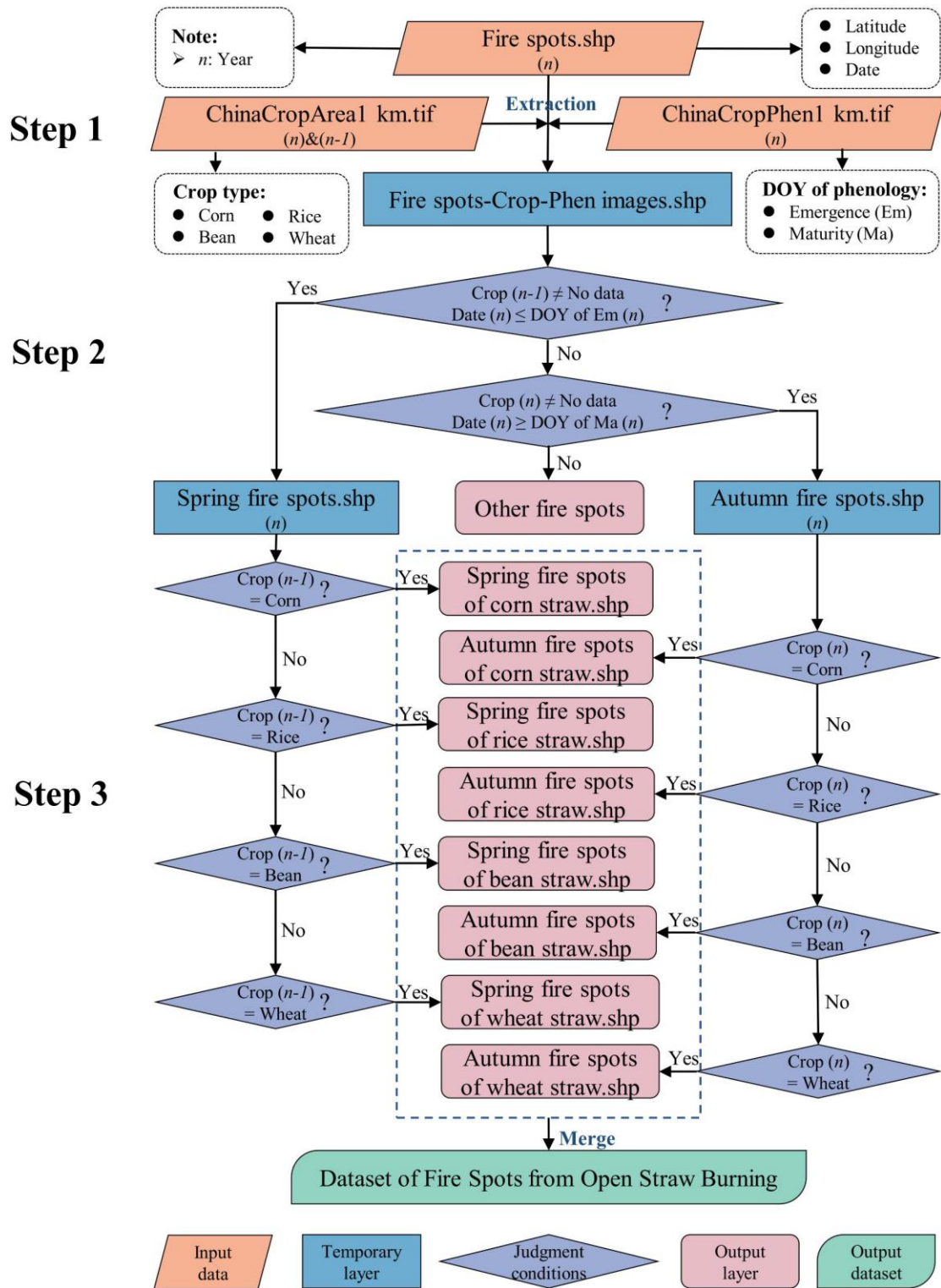
225

226   **Fig. 1** Extraction and classification method for fire spots from open straw burning

227 **2.2 Development of high spatial resolution annual emission inventories for**

228 **GHGs and exploration of driving factors**

229 Annual emission inventories for GHGs were developed for the region of Northeast

230 China at a grid resolution of 5 km × 5 km for the years of 2001 to 2020. The domain

231 grids were created using Fishnet of ArcGIS 10.2 software.

232

233 The modified FRP algorithm (Yang et al., 2020) is used to estimate the emissions of

234 GHGs from open straw burning in this study:

235 $$E = \alpha \times \int_{t_1}^{t_2} FRP^* dt \times \beta \times F = \alpha \times FRP \times f_{FRP} \times (t_2 - t_1) \times \beta \times F \qquad (1)$$

236 where E (in g) is the emissions of GHGs; α is a correction factor used to adjust for FRP

237 detection errors between MODIS and VIIRS, which is given a value of 2.5 following

238 Vadrevu and Lasko (2018), indicating that the FRP VIIRS sum is 2.5 times of the FRP

239 MODIS sum; t_1 and t_2 are the beginning and ending time of fire spots, respectively, and

240 the average burning time (3 hours) of a fire spot in Northeast China was obtained by

241 delivering questionnaires to local farmers (Yang et al., 2020); FRE^* (in MW) is adjusted

242 satellite detected FRP; FRP (in MW) is the instantaneous FRP observed by satellite;

243 f_{FRP} is a correction factor that is used to adjust the underestimated emissions by fire

244 spots, and Yang et al. (2020) determined an optimal value of 5 for f_{FRP} by calibrating

245 the contributions of open straw burning to ground observation data in Northeast China

246 using WRF-CMAQ; β (in kg·MJ^{-1}) is biomass combustion rate and the average value

247 of 0.411 kg·MJ^{-1} from previous studies is used here (Wooster et al., 2005; Freeborn et

248 al., 2008); and F (in $g \cdot kg^{-1}$) is the emission factor for individual straw type (**Table 1**)

249 (Li et al., 2007; Liu et al., 2011; Peng et al., 2016).

250

251 **Table 1.** Emission factors of open straw burning for different crop types

Crop	Emission factors ($g \cdot kg^{-1}$)		
	CO_2	CH_4	N_2O
Corn	1350	4.4	0.12
Rice	1460	3.2	0.11
Bean	1445	3.9	0.09
Wheat	1460	3.4	0.05

252

253 Driving factors such as the output of major grains and rural residential coal

254 consumption for temporal variations of annual GHGs emissions were explored through

255 Pearson correlation analysis using SPSS 20.0. Information on the above data is also

256 detailed in **Table S1**.

257 **3 Results and discussion**

258 **3.1 Spatial and temporal distributions of fire spots**

259 Cultivated lands in Northeast China primarily distribute in Sanjiang Plain (Northeast

260 Heilongjiang Province), Songnen Plain (West Heilongjiang Province and Midwest Jilin

261 Province), and Liao River Plain (Central Liaoning Province) (**Fig. 2(a)**). Fire spots were

262 widely spread, covering most cultivated lands, including both dry and paddy fields

263 across Northeast China (**Fig. 2(a)** and **2(b)**). A total of 156,044 fire spots from open

264 straw burning were recorded during 2001-2020. Note that the traditional method

265   overestimated the total number of fire sports by 7190 over the 20-year period, with the

266   largest in 2017 (an overestimation of 4060) (**Fig. 2(c)**). This highlights the importance

267   of integrating crop cycle information into fire spot extraction for open straw burning to

268   enhance data accuracy and reliability. Considering the 20-year together (2001-2020),

269   high occurrence frequencies of open straw burning (also referred to as intensity of fire

270   spots below) appeared in the northern Sanjiang Plain, eastern Songnen Plain, and

271   eastern Liao River Plain, as well as scattered areas close to Inner Mongolia (**Fig. 2(a)**

272   and **2(b)**).

273

274   Interannual variations of fire spots distributions are shown in **Fig. S1**. In the Sanjiang

275   Plain, low occurrence frequencies of fire spots were observed in a few cultivated lands

276   during 2003-2006 (**Fig. S1(c)** to **Fig. S1(f)**) and in most cultivated lands in the northern

277   part of the Plain during 2007-2013 (**Fig. S1(g)** to **Fig. S1(m)**). Note that in 2014 and

278   later years, fire spots were extended to the entire Sanjiang Plain, and the northern part

279   of the Plain became an area with high intensity of fire spots (**Fig. S1(n)** to **Fig. S1(q)**),

280   although a few cultivated lands in this Plain recorded low intensity of fire spots after

281   2018 (**Fig. S1(r)** to **Fig. S1(t)**). In the Songnen Plain, most cultivated lands recorded

282   fire spots during 2014 to 2017, with highest intensity in the northern and eastern parts

283   of the Plain (**Fig. S1(n)** to **Fig. S1(q)**). The occurrence frequencies of fire spots

284   decreased across the plain since 2018, particularly in the northern part of the Plain (**Fig.**

285   **S1(r)** to **Fig. S1(t)**). In the Liao River Plain, although fire spots were observed in most

286   cultivated lands in the eastern part of the Plain during 2014-2017, high occurrence

287   frequency was only recorded in 2014 (**Fig. S1(n)** to **Fig. S1(q)**).

288

289   Apparently, open straw burning events decreased in all of the three Plains since 2018

290   (**Fig. S1(r)** to **Fig. S1(t)**), which was likely due to the intensified effort from the Chinese

291   government banning open straw burning (Hong et al., 2023). The reduction in the

292   number of fire spots was more significant in the Sanjiang Plain and northern Songnen

293   Plain than Liao River Plain (**Fig. S1**), indicating more compliance with straw burning

294   bans from State Farms in the former two regions.

295
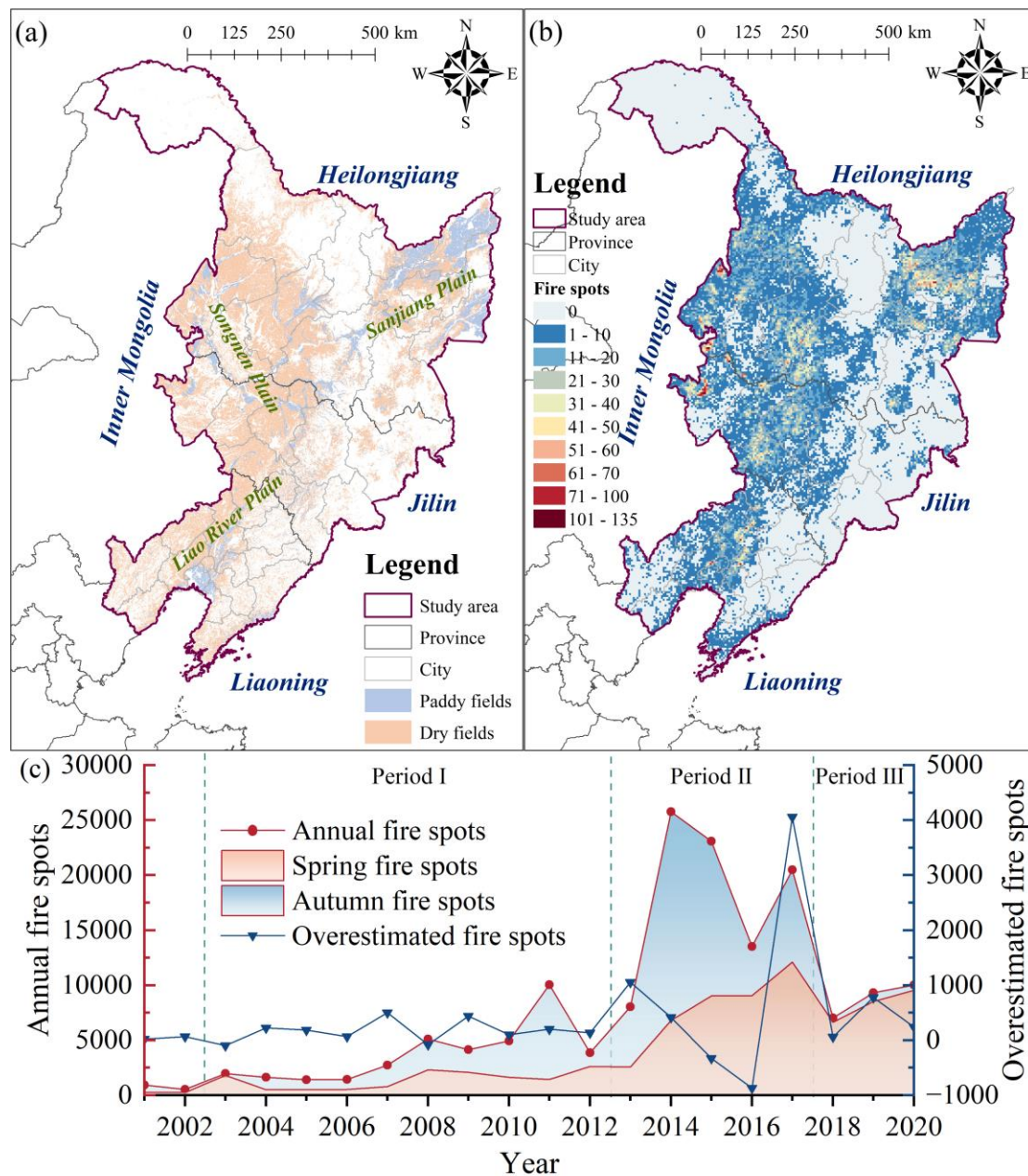
Fig. 2 (a) Spatial distributions of cultivated land in 2020 in Northeast China (https://www.resdc.cn), (b) spatial distributions of the total number of fire spots during 2001-2020 in Northeast China, and (c) seasonal distributions of the annual fire spots, and annual overestimated fire spots by the traditional method from 2001 to 2020. The overestimated fire spots are calculated as the number of fire spots identified by the traditional method minus those extracted by the novel method.

302

Fire spots from open straw burning concentrated in spring and autumn, with few burning events in the other two seasons in Northeast China. Open straw burning events in this region during 2003-2020 can be roughly divided into three distinctive periods (**Fig. 2(c)**). During **Period I** (2003-2012), the annual average number of fire spots in this region was 3732. There were more fire spots in autumn than spring in most of these years. During **Period II** (2013-2017), there was a substantial surge in fire spots, with an annual average of 18,177 spots, accounting for 58.2% of the 20-year total. Notably, the number of fire spots peaked at 25,759 in 2014. Spring fire spots consistently increased annually, reaching the highest in 2017 at 12,094 spots. The variations for autumn fire spots were fluctuating, with a peak of 18,951 spots in 2014. During 2013-2015, autumn fire spots were higher than spring; however, this trend reversed in 2016 and 2017, with spring fire spots becoming more dominant. During **Period III** (2018-2020), the number of fire spots experienced a significant decrease, averaging 8,788 spots annually, which was a 51.7% decrease from **Period II**. Spring emerged as the primary season of fire spots, accounting for approximately 93.8% of the annual total. Zhao et al. (2021) have reported a similar phenomenon, in which the primary season of open straw burning in Northeast China gradually shifts to spring (April to June). The apparent seasonal variations of open straw burning primarily stems from strict government bans imposed after the autumn harvest (Yang et al., 2020). In addition, farmers' increasing awareness regarding how open straw burning contributes

323   to the thawing of spring soil may also be a factor (Saxton et al., 1993; Song et al., 2024).

324

325   However, the "sudden drop" in fire spots should also be partially attributed to strategies

326   employed by farmers to avoid detection by satellite and government regulations, such

327   as burning straw on smaller scales and in more dispersed areas, or during non-transit

328   times of the satellites (Liu et al. 2019; Liu et al. 2020). Chen et al. (2022) also found

329   that farmers in East China frequently burned straw in 2019 during non-transit times of

330   MODIS/VIIRS satellites, as indicated by Himawari satellite data. To further verify the

331   reliability of the "sudden drop" in fire spots in Northeast China, we analyzed the trend

332   of particulate matter concentrations (PM_{10} and $PM_{2.5}$) during the periods of open straw

333   burning from 2014 to 2020 in Northeast China (**Fig. S2**). Atmospheric particulate

334   matter concentrations during autumn open straw burning in Northeast China decreased

335   with a "sudden drop" in fire spots (**Fig. S2(c)**). However, a similar trend was not

336   observed in spring (**Fig. S2(b)**), possibly due to limitations in fire spot detection by

337   current satellite techniques and avoidance strategies. Kumar et al. (2021) suggested that

338   a hybrid inventory, which accurately allocates emissions estimated using the "bottom-

339   up" approach based on satellite data, may be more advantageous in this scenario.

340

341   The straw burning dates in Northeast China also changed during the three periods,

342   besides varying with crop type. During **Period I** (2003-2012), the autumn burning dates

343   of corn and rice straws were concentrated from early October to mid-November (DOY

344   range of 270 to 320). Spring burning dates of corn and rice straw were concentrated

345   between mid-March and late April (DOY range of 70 to 120) in 2003, while dispersed

346   to early March to mid-May (DOY range of 60 to 140) in 2012 (**Fig. 3(a)** and **Fig. 3(b)**).

347   During **Period II** (2013-2017), the dispersion of spring burning dates for corn and rice

348   straws became more pronounced, extending from early February to mid-May (DOY

349   range of 30 to 140) (**Fig. 3(a)** and **Fig. 3(b)**). During **Period III** (2018-2020), the

350   dispersion of spring burning dates for corn and rice straws persisted (**Fig. 3(a)** and **Fig.**

351   **3(b)**). During **Period I** (2003-2012), the spring and autumn burning dates of bean straw

352   in Heilongjiang Province were concentrated from mid-March to late April (DOY range

353   of 70 to 120) and from early October to mid-November (DOY range of 270 to 320),

354   respectively (**Fig. 3(c)**). During 2013-2020, the spring burning dates of bean straw in

355   Northeast China were concentrated between early February and late April (DOY range

356   of 30 to 120), while the autumn burning dates remained consistent with those during

357   **Period I** in Heilongjiang Province (**Fig. 3(c)**). Unlike other crops, the burning dates for

358   wheat straw did not conform to the aforementioned pattern of variation, likely due to a

359   limited number of fire spots (**Fig. 3(d)**). The changing dispersion of burning dates for

360   each crop type indicates shifts in agricultural practices that may be influenced by

361   regional straw burning ban policies, environmental conditions, and farming practices

362   (Yang et al., 2020).

363
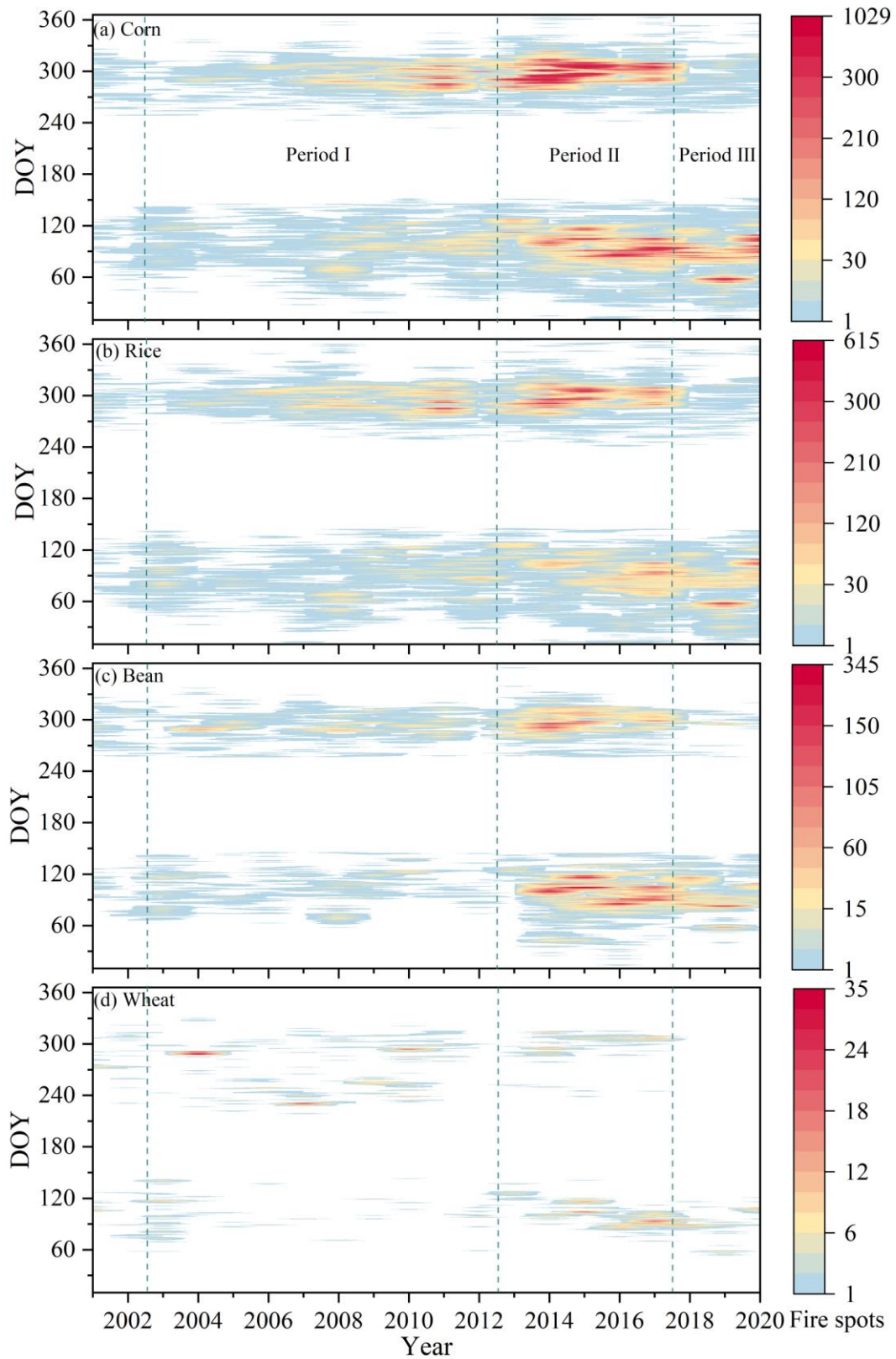
Fig. 3 The daily frequency distribution of fire spots from various straws burning: (a), (b), (c),

and (d) represent corn, rice, bean, and wheat straw, respectively. Note: The x-axis is Year; the

366 y-axis is DOY; and the range of colorbars (indicating fire spots) is different for each crop, with

367 values ranging from 1 to 1,029 for corn, 1 to 615 for rice, 1 to 345 for beans, and 1 to 35 for

368 wheat.

369 **3.2 High spatial resolution annual emission inventory of GHGs**

370 The cumulative emissions of CO_2, CH_4, and N_2O from open straw burning in Northeast

371 China from 2001 to 2020 amounted to 198 Tg, 557 Gg, and 15.7 Gg, respectively (or

372 218 Tg CO_2-eq in total). The spatial distributions of GHGs emissions correspond well

373 with those of fire spots, particularly in high emission areas (**Fig. 2** and **Fig. 4**). However,

374 the amounts of GHGs emissions in the northern Songnen Plain unexpectedly exceeded

375 those in the eastern Songnen Plain and eastern Liao River Plain, suggesting that even

376 low intensity fire spots can generate considerable emissions of GHGs due to higher

377 FRP detected via remote sensing. Therefore, the FRP algorithm proves to be more

378 effective than burned areas-based algorithms in identifying emission intensity resulted

379 from open straw burning while reducing the uncertainty associated with high

380 spatiotemporal resolution emission inventory (Wu et al., 2023).

381

382 The annual emissions of CO_2, CH_4, N_2O, and CO_2-eq from 2001 to 2020 are presented

383 in **Figs**. **S3**, **S4**, **S5**, and **S6**, respectively. The spatiotemporal patterns of GHGs

384 emissions correspond well to the observed trends in fire spots during **Period I** (2003-

385 2012). However, during **Period II** (2013-2017) and **Period III** (2018-2020), the

386 emissions of GHGs in the eastern Songnen Plain and eastern Liao River Plain did not

387   exhibit a proportional increase with the rise in fire spots. This discrepancy can be

388   attributed to the dispersed burning dates among individual farmers in these regions,

389   resulting in high intensity fire spots with relatively low emissions. In contrast, several

390   State Farms located in the northern Sanjiang Plain and northern Songnen Plain

391   demonstrated a higher level of synchronization in open straw burning activities,

392   resulting in parallel trends between fire spots and emissions (Cui et al., 2021).

393
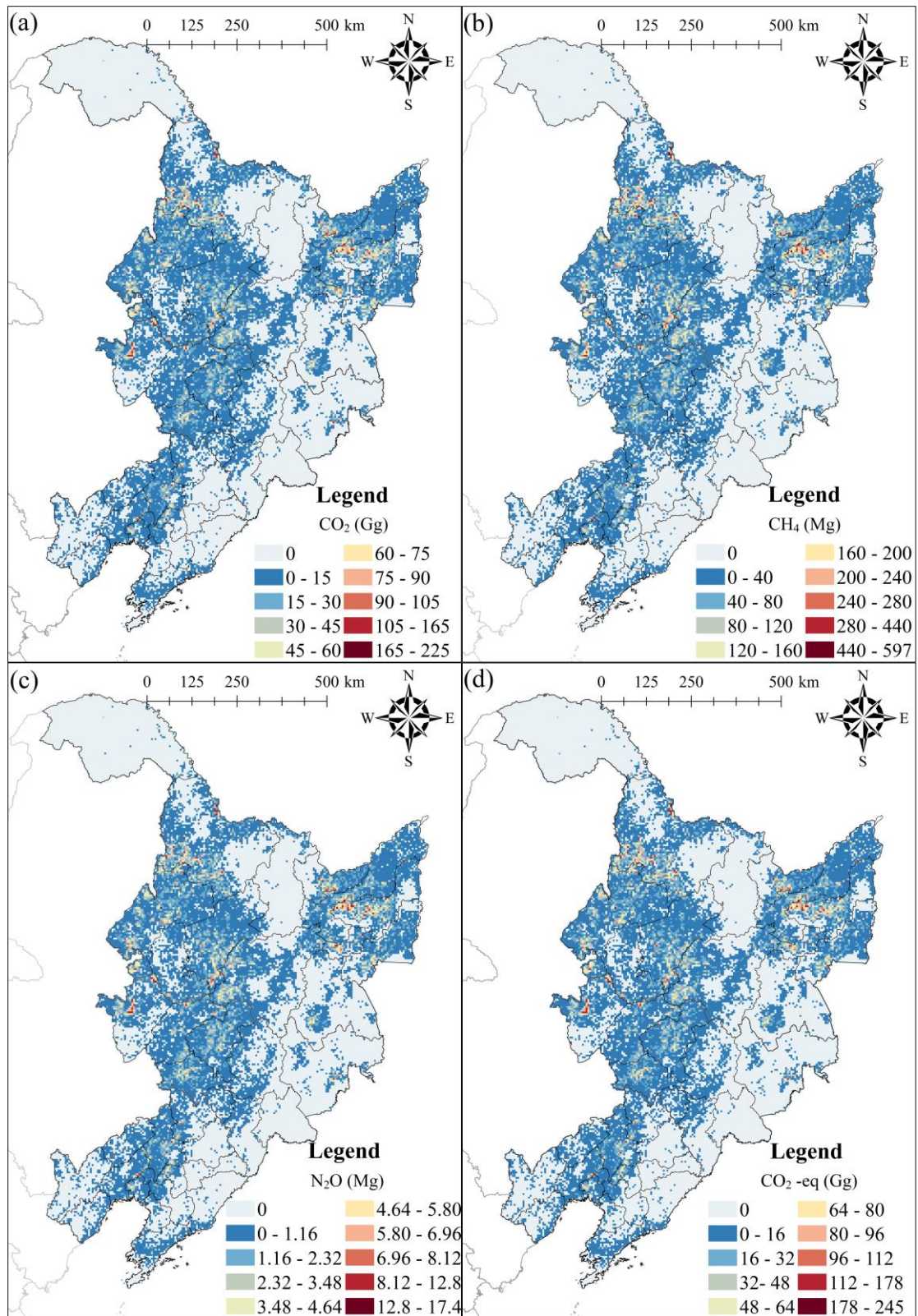
Fig. 4 The cumulative GHGs emissions from open straw burning in Northeast China from 2001

to 2020 for CO_2 (a), CH_4 (b), N_2O (c), and CO_2-eq (d) emissions, respectively. Note: The range

of colorbars (indicating emissions) is different for each GHG, with values ranging from 0 to

397   225 Gg for CO_2, 0 to 597 Mg for CH_4, 0 to 17.4 Mg for N_2O, and 0 to 245 Gg for CO_2-eq.

398

399   During **Period I** (2003 - 2012), average annual CO_2-eq emission was at 4.20 Tg, and

400   the cumulative CO_2-eq emission amounted to 42.0 Tg. During **Period II** (2013 - 2017),

401   average annual CO_2-eq emission increased substantially to 26.1 Tg, and the cumulative

402   emission during this period amounted to 130 Tg, which accounted for 59.9% of the total

403   emissions over the two decades. During **Period III** (2018 - 2020), average annual CO_2-

404   eq emissions decreased significantly to 14.3 Tg, and the cumulative emission during

405   this period amounted to 42.8 Tg (**Fig. 5(a)**). The trend of CO_2-eq emission from 2003

406   to 2020 generally corresponds with the occurrence of fire spots, except for 2015 when

407   higher emissions were obtained despite having fewer fire spots than the case in 2014

408   (**Fig. 5(a)**). Such a trend is consistent with those of carbonaceous gases and aerosols

409   (CGA) emissions estimated by Liu et al., (2022). This discrepancy between fire spots

410   and pollutant emissions in 2015 highlights the limitations of estimating pollutant

411   emissions based solely on burned areas (Ke et al., 2019; Wu et al. 2023). The

412   combustion of corn and rice straw was identified as the primary contributors to CO_2-eq

413   emissions, accounting for 51.1% and 30.8%, respectively, of the total emissions (**Fig.**

414   **5(b)**). Specifically, corn straw burning released 99.6, 9.06, and 2.42 Tg, while rice straw

415   burning released 61.8, 3.78, and 1.27 Tg of CO_2, CO_2-eq for CH_4, and CO_2-eq for N_2O,

416   respectively.

417

418
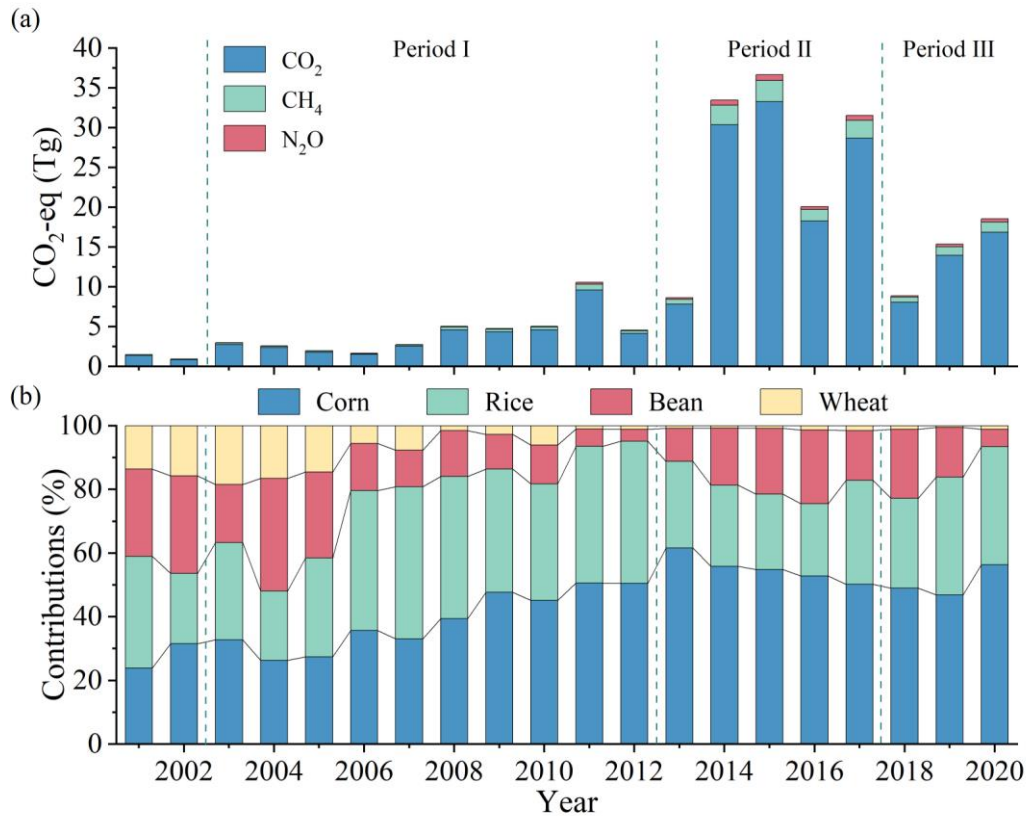
Fig. 5 (a) Regional total annual CO_2-eq emissions and (b) percentage contributions from open

420   burning of individual crop straw type.

421   **3.3 Validation and limitations**

422   Our estimated total CO_2 emissions from 2012 to 2020 with MODIS (161 Tg) or with

423   VIIRS (165 Tg) were much lower than that (~ 523 Tg) estimated by Liu et al. (2022),

424   the latter was based on a modified FRP algorithm and fire spot products by VIIRS,

425   which has limitations in its traditional straw extraction methods in accurately

426   identifying fire spots during certain times of the year. Our estimated CO_2 emission from

427   2002 to 2020 in Northeast China (196 Tg) was slightly lower than that (195 Tg)

428   estimated by Global Fire Emissions Database Version 4.1 (GFED4.1s) by van der Werf et al.

429   (2017), and slightly higher than that (181 Tg) estimated from the Fire Inventory from

430 NCAR version 2.5 (FINNv2.5) by Wiedinmyer et al. (2023), which addresses the

431 underestimation of open biomass burning in China by the older version FINNv1.5

432 (Stavrakou et al., 2016; Yang et al., 2020) (**Fig. 6**). However, our estimated total CO_2

433 emission from 2012 to 2020 was significantly higher than that (35.6 Tg) estimated by

434 VIIRS-based Fire Emission Inventory version 0 (VFEIv0) by Ferrada et al. (2022),

435 which relies on the traditional FRP algorithm (**Fig. 6**). Furthermore, Northeast China

436 surpassed East China (27.1 Tg) as the highest emitter from open straw burning in China

437 since 2014, with CO_2 emissions reaching 30.4 Tg (Zhang et al. 2020).
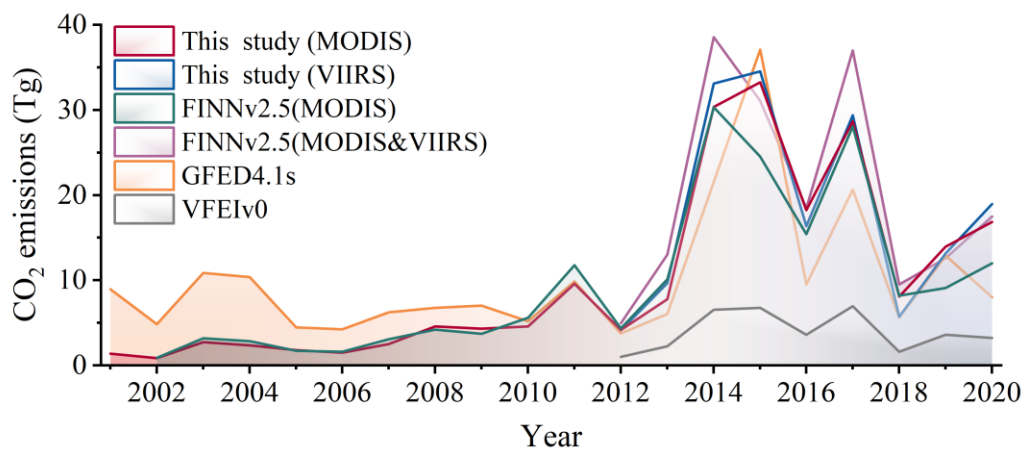
438

439 **Fig. 6** Annual total emissions of CO_2 from open straw burning (agricultural waste burning) in

440 Northeast China from this study with MODIS (red, 2001-2020) and VIIRS (blue, 2012-2020),

441 the Fire Inventory from NCAR version 2.5 (FINNv2.5) with MODIS-only (green, 2002-2020),

442 FINNv2.5 with MODIS and VIIRS (purple, 2012-2020), Global Fire Emissions Database

443 Version 4.1 (GFED4.1s) (orange, 2001-2020), and VIIRS-based Fire Emission Inventory

444 version 0 (VFEIv0) (grey, 2012-2020).

445

446 Although this study effectively improved the accuracy of emission inventory for open

447   straw burning through the novel method that integrates crop cycle information into

448   extraction and classification of fire spots and the modified FRP algorithm, certain

449   limitations still exist. The uncertainty in this study stems mainly from the inherent

450   limitations of satellite fire detection systems. The MODIS fire spot product, although

451   widely used, is limited by its temporal resolution and tends to miss transient or small-

452   scale fires. In addition, straw burning during non-satellite transit periods, on cloudy

453   days, at night, and under heavy haze further exacerbates the underestimation of fire

454   incidence, leading to potential gaps in emission inventories.

455

456   Additionally, the novel method that integrates crop cycle information into extraction

457   and classification of fire spots presents a promising advancement. However, its

458   applicability is constrained to regions where comprehensive and detailed crop data are

459   available. In countries or regions lacking such agricultural information, this method

460   may face challenges, thereby limiting its broader applicability. These factors underscore

461   the need for continued refinement of satellite detection technologies and the expansion

462   of agricultural data collection efforts to reduce uncertainties and enhance the robustness

463   of emission inventories on regional to global scales.

464   **3.4 Driving factors of open straw burning**

465   Open straw burning is more prominently influenced by anthropogenic activities

466   compared to other types of open biomass burning, such as forest, shrubland, and

467   grassland fires (Syphard et al., 2017; Wu et al., 2020). Open straw burning is influenced

468 by changes in straw yield and utilization rate, straw burning ban policy, and farmers'

469 awareness of straw burning consequences (Chen et al., 2016; Li et al., 2017; Tao et al.,

470 2018; Fang et al., 2019; Xu et al., 2023b).

471

472 Northeast China has experienced a remarkable expansion in its sown area for major

473 grain crops over the past two decades. By 2020, the sown area reached 231,937 km^2,

474 61.4% more than that in 2001 (National Bureau of Statistics of China, 2002-2021). In

475 the meantime, annual straw yield reached 143 Tg in 2020, 142% higher than that (59.2

476 Tg) in 2001 (**Fig.7**) (numbers are calculated based on the major grain yields in

477 Northeast China presented in National Bureau of Statistics of China (2002-2021) and

478 the ratio of straw and grain (Wang et al.,2012)). Note that the annual straw yields have

479 stabilized around 140 Tg since 2017, and this trend is expected to persist for many years

480 to come (**Fig. 7**). From 2003 to 2020, a strong positive correlation was observed

481 between the straw yields and the emissions of CO_2-eq from open straw burning across

482 Northeast China, as well as in Heilongjiang and Jilin provinces ($p < 0.01$, **Table S2**). If

483 looking at individual periods, significant correlations were only observed during

484 **Period I** (2003-2012) for the whole of Northeast China ($p < 0.01$) and Heilongjiang (p

485 < 0.01) (**Table S2**). This highlights that increased straw yields exacerbated the

486 challenges of straw disposal in Northeast China and have been a major contributor to

487 the increase in the emissions of GHGs from open straw burning in the aforementioned

488 region and period.

489

Besides open burning, crop straw is also used for cooking and heating in rural households in Northeast China (Ke et al., 2023; Liu et al., 2023). Crop straw can also be converted to bioenergy, used as animal feed, and returned to the fields (Alengebawy et al., 2022; Fang et al., 2022). However, exact quantification of straw utilization in different sectors in Northeast China is still lacking (Shi et al., 2023). Knowing that coal combustion and straw burning are major energy sources for rural households in Northeast China, we tried to explore potential changes in straw utilization on open straw burning through coal consumption changes (Fang et al. 2019). The abrupt increase in rural residential coal consumption in 2013 in Northeast China coincided with a spike in CO_2-eq emissions from open straw burning (**Fig. 7(a)**). Furthermore, a significant positive correlation between rural residential coal consumption and CO_2-eq emissions in Northeast China was revealed, especially in Heilongjiang and Jilin provinces (**Table S3**). We thus speculate that the increase in rural commercial energy consumption may have reduced the demand for straw as an energy source for agricultural households, thus facilitating the increased open straw burning. This needs to be confirmed in future studies once various straw utilization pathways are quantified.
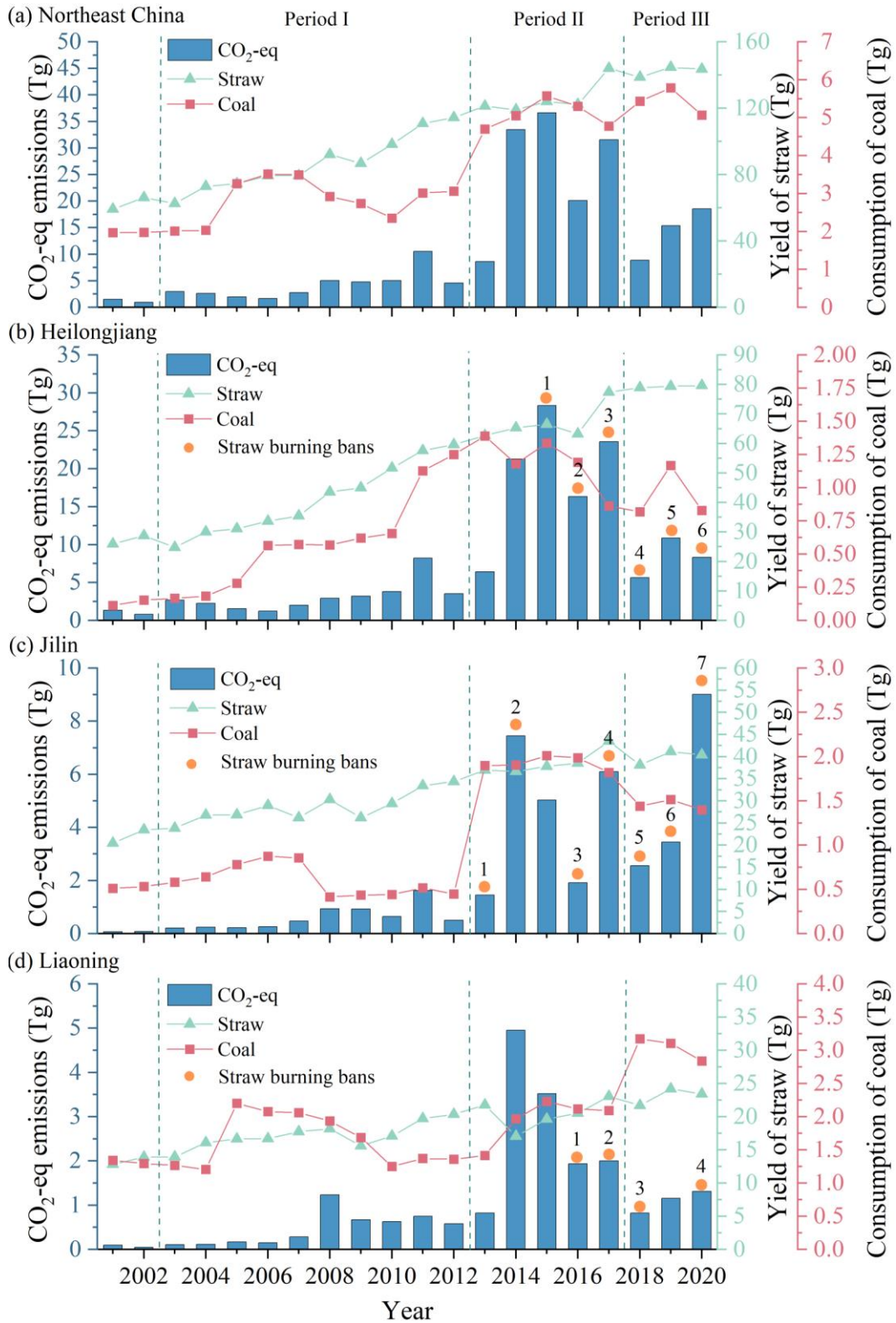
506

507 **Fig. 7** Annual CO$_2$-eq emissions, yield of straw, rural residential coal consumption, and straw

508 burning bans in (a) Northeast China, (b) Heilongjiang, (c) Jilin, and (d) Liaoning from 2001 to

509 2020. Note: The range of y-axis is different for each region. The blue y-axis indicates CO$_2$-eq

emissions, with values ranging from 0 to 50 Tg for Northeast China, 0 to 35 Tg for Heilongjiang, 0 to 10 Tg for Jilin, and 0 to 6 Tg for Liaoning; the green y-axis indicates yield of straw, with values ranging from 0 to 160 Tg for Northeast China, 0 to 90 Tg for Heilongjiang, 0 to 60 Tg for Jilin, and 0 to 40 Tg for Liaoning; and the red y-axis indicates rural residential coal consumption, with values ranging from 0 to 7 Tg for Northeast China, 0 to 2 Tg for Heilongjiang, 0 to 3 Tg for Jilin, and 0 to 4 Tg for Liaoning.

We also evaluated the efficacy of straw burning ban policy in Heilongjiang, Jinlin, and Liaoning (**Table S4**). Despite the implementation of the policy since 2013 in this region, a significant reduction in CO_2-eq emissions from open straw burning was only observed after 2018 (**Fig. 7**). Compared to the other regions of China, the effective control of open straw burning was delayed by several years in Northeast China (Huang et al., 2021). An important phenomenon was observed regarding the geographical and temporal expansion of the ban policy, e.g., initially focused on key areas and specific seasons (autumn and winter) and progressively extended to the entire region and throughout the whole year (see Heilongjiang Province as an example, **Table S4**). Therefore, enhanced enforcement of the ban policy likely reduced CO_2-eq emissions during **Period III** and shifted the burning season to spring.

In conclusion, the enforcement of region-specific straw burning bans tailored to spatiotemporal variations is crucial to control GHGs emissions, given the anticipated

531 sustained high straw yields in the future. Additionally, promoting diverse methods for

532 utilizing straw is highlighted as an effective strategy for mitigating carbon emissions

533 resulted from open straw burning in Northeast China. A combined effort on policy

534 enforcement and alternative straw usage would play a pivotal role in addressing the

535 environmental challenges posed by agricultural practices in the region.

536

537 **4   Conclusions**

538 This study provides a comprehensive analysis of the spatiotemporal variations of open

539 straw burning across Northeast China from 2001 to 2020 and develops regional scale

540 high spatial resolution annual emission inventories of GHGs. Open straw burning in

541 Northeast China emitted a total of 218 Tg of CO_2-eq during 2001-2020, of which 19.3%

542 was from **Period I** (2003-2012), 59.9% from **Period II** (2013-2017), and 19.7% from

543 **Period III** (2018-2020). Analysis results demonstrate the necessity of integrating the

544 crop cycle information into the extraction and classification of fire spots from open

545 straw burning to enhance the accuracy of emission inventories of various pollutants.

546 This study also highlights the inconsistencies between the number of fire spots and

547 pollutant emissions caused by remote sensing detection techniques. In Northeast China,

548 regions such as the northern Sanjiang Plain, eastern and northern Songnen Plain, and

549 eastern Liao River Plain are identified as high-emission areas of GHGs from open straw

550 burning, which emitted 38.1, 45.5, 31.9, and 10.8 Tg of CO_2-eq, respectively, during

2001-2020. Additionally, it is observed that the season for open straw burning has shifted from autumn to spring, with dispersed burning dates. This spatiotemporal analysis provides crucial insights into policy effectiveness as well as geographical variations regarding compliance with regulations banning open straw burning. Consequently, government policies prohibiting open straw burning should be adjusted according to the observed spatiotemporal variations in different regions. Simultaneously promoting diversified applications of straw, such as bioenergy conversion, animal feeding, and soil amendment, is recommended — a strategy that is aligned with China's dual-carbon objectives aiming at achieving carbon peak and carbon neutrality.

Competing interests

At least one of the (co-)authors is a member of the editorial board of Atmospheric Chemistry and Physics.

Acknowledgments

This work was supported by the Distinguished Youth Science Foundation of Heilongjiang Province (JQ2023E001) and Young Leading Talents of Northeast Agricultural University (NEAU2023QNLJ-013).

570

References

572 Ahmed, W., Tan, Q., Ali, S., and Ahmad, N.: Addressing environmental implications of

573 crop stubble burning in Pakistan: innovation platforms as an alternative approach, Int.

574 J. Global Warming, 19, 76-93, https://doi.org/10.1504/IJGW.2019.101773, 2019.

575 Alengebawy, A., Mohamed, B.A., Ran, Y., Yang, Y., Pezzuolo, A., Samer, M., and Ai,

576 P.: A comparative environmental life cycle assessment of rice straw-based bioenergy

577 projects in China, Environ. Res., 212, 113404,

578 https://doi.org/10.1016/j.envres.2022.113404, 2022.

579 Chen, J.X., Li, R., Tao, M.H., Wang, L.L., Lin, C.Q., Wang, J., Wang, L.C., Wang, Y.,

580 Chen, L.F.: Overview of the performance of satellite fire products in China:

581 Uncertainties and challenges, Atmos. Environ., 268, 118838,

582 https://doi.org/10.1016/j.atmosenv.2021.118838, 2022.

583 Chen, Y.L., Shen, H.Z., Zhong, Q.R., Chen, H., Huang, T.B., Liu, J.F., Cheng, H.F.,

584 Zeng, E.Y., Smith, K.R., and Tao, S.: Transition of household cookfuels in China from

585 2010 to 2012, Appl. Energ., 184, 800-809,

586 https://doi.org/10.1016/j.apenergy.2016.07.136, 2016.

587 Cui, S., Song, Z.H., Zhang, L.M., Shen, Z.X., Hough, R., Zhang, Z.L., An, L.H., Fu,

588 Q., Zhao, Y.C., and Jia, Z.Y.: Spatial and temporal variations of open straw burning

589 based on fire spots in northeast China from 2013 to 2017, Atmos. Environ., 244, 117962,

590   https://doi.org/10.1016/j.atmosenv.2020.117962, 2021.

591   Fang, Y.R., Wu, Y., and Xie, G.H.: Crop residue utilizations and potential for bioethanol

592   production in China, Renew. Sust. Energ. Rev., 113, 109288,

593   https://doi.org/10.1016/j.rser.2019.109288, 2019.

594   Fang, Y.R., Zhang, S.L., Zhou, Z.Q., Shi, W.J., and Xie, G.H.: Sustainable development

595   in China: Valuation of bioenergy potential and CO_2 reduction from crop straw, Appl.

596   Energ., 322, 119439, https://doi.org/10.1016/j.apenergy.2022.119439, 2022.

597   Ferrada, G.A., Zhou, M., Wang, Jun., Lyapustin, A., Wang, Y.J., Freitas, S.R., and

598   Carmichael, G.R.: Introducing the VIIRS-based Fire Emission Inventory version 0

599   (VFEIv0), Geosci. Model Dev., 15, 8085-8109, https://doi.org/10.5194/gmd-15-8085-

600   2022, 2022.

601   Freeborn, P.H., Wooster, M.J., Hao, W.M., Ryan, C.A., Nordgren, B.L., Baker, S.P., and

602   Ichoku, C.: Relationships between energy release, fuel mass loss, and trace gas and

603   aerosol emissions during laboratory biomass fires, J. Geophys. Res-Atmos., 113,

604   D01301, https://doi.org/10.1029/2007JD008679, 2008.

605   Fu, J., Song, S.T., Guo, L., Chen, W.W., Wang, P., Duanmu, L.J., Shang, Y.J., Shi, B.W.,

606   and He, L.Y.: Interprovincial joint prevention and control of open straw burning in

607   Northeast China: Implications for atmospheric environment management, Remote

608   Sens., 14(11), 2528, https://doi.org/10.3390/rs14112528, 2022.

609   Gadde, B., Bonnet, S., Menke, C., and Garivait, S.: Air pollutant emissions from rice

610   straw open field burning in India, Thailand and the Philippines, Environ. Pollut., 157,

1554-1558, https://doi.org/10.1016/j.envpol.2009.01.004, 2009.

Giglio, L., Schroeder, W., and Justice, C.O.: The collection 6 MODIS active fire detection algorithm and fire products, Remote Sens. Environ., 178, 31-41, https://doi.org/10.1016/j.rse.2016.02.054, 2016.

Guan, Y.N., Chen, G.Y., Cheng, Z.J., Yan, B.B., and Hou, L.A.: Air pollutant emissions from straw open burning: A case study in Tianjin, Atmos. Environ., 171, 155-164, https://dx.doi.org/10.1016/j.atmosenv.2017.10.020, 2017.

Hong, X., Zhang, C., Tian, Y., Wu, H., Zhu, Y., and Liu, C.: Quantification and evaluation of atmospheric emissions from crop residue burning constrained by satellite observations in China during 2016-2020, Sci. Total. Environ., 865, 161237, https://doi.org/10.1016/j.scitotenv.2022.161237, 2023.

https://modis-fire.umd.edu/files/MODIS_C61_BA_User_Guide_1.1.pdf

https://modis-fire.umd.edu/files/MODIS_C6_C6.1_Fire_User_Guide_1.0.pdf

Huang, K., Zhuang, G., Lin, Y., Wang, Q., Fu, J.S., Fu, Q., Liu, T., and Deng, C.: How to improve the air quality over megacities in China: pollution characterization and source analysis in Shanghai before, during, and after the 2010 World Expo, Atmos. Chem. Phys., 13, 5927-5942, https://doi.org/10.5194/acp-13-5927-2013, 2013.

Huang, L., Zhu, Y.H., Liu, H.Q., Wang, Y.J., Allen, D.T., Ooi, M.C.G., Manomaiphiboon, K., Latif, M.T., Chan, A., and Li, L.: Assessing the contribution of open crop straw burning to ground-level ozone and associated health impacts in China and the effectiveness of straw burning bans, Environ. Int., 171, 107710,

https://doi.org/10.1016/j.envint.2022.107710, 2023.

Huang, L., Zhu, Y.H., Wang, Q., Zhu, A.S., Liu, Z.Y., Wang, Y.J., Allen, D.T., and Li, L.: Assessment of the effects of straw burning bans in China: Emissions, air quality, and health impacts, Sci. Total Environ., 789, 147935, https://doi.org/10.1016/j.scitotenv.2021.147935, 2021.

Huang, X., Li, M.M., Li, J.F., and Song, Y.: A high-resolution emission inventory of crop burning in fields in China based on MODIS Thermal Anomalies/Fire products, Atmos. Environ., 50, 9-15, https://doi.org/10.1016/j.atmosenv.2012.01.017, 2012.

Jin, Q., Ma, X., Wang, W., Yang, S., and Guo, F.: Temporal and spatial variations of $PM_{2.5}$ emissions from crop straw burning in eastern China during 2000-2014. Acta Sci. Circumstantiae, 37, 460-468, 2017. (in Chinese)

Jin, Q.F., Ma, X.Q., Wang, G.Y., Yang, X.J., and Guo, F.T.: Dynamics of major air pollutants from crop residue burning in mainland China, 2000-2014, J. Environ. Sci., 70, 190-205, https://doi.org/10.1016/j.jes.2017.11.024, 2018.

Ke, H.B., Gong, S.L., He, J.J., Zhou, C.H., Zhang, L., and Zhou, Y.K.: Spatial and temporal distribution of open bio-mass burning in China from 2013 to 2017, Atmos. Environ., 210, 156-165, https://doi.org/10.1016/j.atmosenv.2019.04.039, 2019.

Ke, Y.X., Zhang, F.X., Zhang, Z.L., Hough, R., Fu, Q., Li, Y.F., and Cui, S.: Effect of combined aging treatment on biochar adsorption and speciation distribution for Cd (II), Sci. Total Environ., 867, 161593, http://doi.org/10.1016/j.scitotenv.2023.161593, 2023.

Korontzi, S., McCarty, J., Loboda, T., Kumar, S., and Justice, C.: Global distribution of

653   agricultural fires in croplands from 3 years of Moderate Resolution Imaging

654   Spectroradiometer (MODIS) data, Global Biogeochem. Cy., 20, GB2021,

655   https://doi.org/10.1029/2005GB002529, 2006.

656   Kumar, A., Hakkim, H., Sinha, B., and Sinha, V.: Gridded 1 km × 1 km emission

657   inventory for paddy stubble burning emissions over north-west India constrained by

658   measured emission factors of 77 VOCs and district-wise crop yield data, Sci. Total

659   Environ., 789, 48064, https://doi.org/10.1016/j.scitotenv.2021.

660   148064, 2021.

661   Li, C.L., Hu, Y.J., Zhang, F., Chen, J.M., Ma, Z., Ye, X.N., Yang, X., Wang, L., Tang,

662   X.F., Zhang, R.H., Mu, M., Wang, G.H., Kan, H.D., Wang, X.M., and Mellouki, A.:

663   Multi-pollutant emissions from the burning of major agricultural residues in China and

664   the related health-economic effects, Atmos. Chem. Phys., 17, 4957-4988,

665   https://doi.org/10.5194/acp-17-4957-2017, 2017.

666   Li, X.H., Wang, S.X., Duan, L., Hao, J.M., Li, C., Chen, Y.S., and Yang, L.: Particulate

667   and trace gas emissions from open burning of wheat straw and corn stover in China,

668   Environ. Sci. Technol., 41(17), 6052-6058, https://doi.org/10.1021/es0705137, 2007.

669   Li, X.Y., Yu, L., Peng, D.L., and Gong, P.: A large-scale, long time-series (1984-2020)

670   of soybean mapping with phenological features: Heilongjiang Province as a test case,

671   Int. J. Remote Sens., 42, 7332-7356, https://doi.org/10.1080/01431161.2021.1957177,

672   2021.

673   Liu, L.H., Jiang, J.Y., and Zong, L.G.: Emission inventory of greenhouse gases from

674   agricultural residues combustion: A case study of Jiangsu Province, Environ. Sci., 32,

675   1242-1248, 2011. (In Chinese)

676   Liu, T.J., Marlier, M.E., Karambelas, A., Jain, M., Singh, S., Singh, M.K., Gautam, R.,

677   DeFries, R.S.: Missing emissions from post-monsoon agricultural fires in northwestern

678   India: regional limitations of MODIS burned area and active fire products, Environ.

679   Res. Commun., 1, 011007, https://doi.org/10.1088/2515-7620/ab056c, 2019.

680   Liu, T.J., Mickley, L.J., Singh, S., Jain, M., DeFries, R.S., Marlier, M.E.: Crop residue

681   burning practices across north India inferred from household survey data: Bridging

682   gaps in satellite observations, Atmos. Environ. - X, 8, 100091,

683   https://doi.org/*118838*10.1016/j.aeaoa.2020.100091, 2020.

684   Liu, Y.X., Zhao, H.M., Zhao, G.Y., Zhang, X.L., and Xiu, A.J.: Carbonaceous gas and

685   aerosol emissions from biomass burning in China from 2012 to 2021, J. Clean. Prod.,

686   362, 132199, https://doi.org/10.1016/j.jclepro.2022.132199, 2022.

687   Liu, Y.Z., Zhang, J., and Zhuang, M.H.: Bottom-up re-estimations of greenhouse gas

688   and atmospheric pollutants derived from straw burning of three cereal crops production

689   in China based on a national questionnaire, Environ. Sci. Pollut. Res., 28, 65410-65415,

690   https://doi.org/10.1007/s11356-021-15658-9, 2021.

691   Liu, Z.K., Cui, S., Fu, Q., Zhang, F.X., Zhang, Z.L., Hough, R., An, L.H., Li, Y.F., and

692   Zhang, L.M.: Transport of neonicotinoid insecticides in a wetland ecosystem: has the

693   cultivation of different crops become the major sources? J. Environ. Manag. 339,

694   117838, https://doi.org/10.1016/j.scitotenv.2023.161593, 2023.

695 Luo, Y.C., Zhang, Z., Li, Z.Y., Chen, Y., Zhang, L.L., Cao, J., and Tao, F.L.: Identifying

696 the spatiotemporal changes of annual harvesting areas for three staple crops in China

697 by integrating multi-data sources. Environ. Res. Lett., 15, 074003,

698 https://doi.org/10.1088/1748-9326/ab80f0, 2020a.

699 Luo, Y.C., Zhang, Z., Chen, Y., Li, Z.Y., and Tao, F.L.: ChinaCropPhen1km: a high-

700 resolution crop phenological dataset for three staple crops in China during 2000-2015

701 based on leaf area index (LAI) products, Earth Syst. Sci. Data, 12, 197-214,

702 https://doi.org/10.5194/essd-12-197-2020, 2020b.

703 Lv, Q.C., Yang, Z.Y., Chen, Z.Y., Li, M.C., Gao, B.B., Yang, J., Chen, X., and Xu, B.:

704 Crop residue burning in China (2019-2021): Spatiotemporal patterns, environmental

705 impact, and emission dynamics, Env. Sci. Ecotechnol., 21, 100394,

706 https://doi.org/10.1016/j.ese.2024.100394, 2024.

707 Mehmood, K., Wu, Y.J., Wang, L.Q., Yu, S.C., Li, P.F., Chen, X., Li, Z., Zhang Y.B., Li,

708 M.Y., Liu, W.P., Wang, Y.S., Liu, Z.R., Zhu, Y.N., Rosenfeld, D., and Seinfeld, J.H.:

709 Relative effects of open biomass burning and open crop straw burning on haze

710 formation over central and eastern China: modeling study driven by constrained

711 emissions, Atmos. Chem. Phys., 20, 2419-2443, https://doi.org/10.5194/acp-20-2419-

712 2020, 2020.

713 National Bureau of Statistics of China (NBSC): China Statistical Yearbook, China

714 Statistics Press, Beijing, http://www.stats.gov.cn/sj/ndsj/, 2002-2021. (in Chinese)

715 Pan, X.L., Kanaya, Y., Taketani, F., Miyakawa, T., Inomata, S., Komazaki, Y., Tanimoto,

716   H., Wang, Z., Uno, I., and Wang, Z.F.: Emission characteristics of refractory black

717   carbon aerosols from fresh biomass burning: a perspective from laboratory experiments,

718   Atmos. Chem. Phys., 17, 13001-13016, https://doi.org/10.5194/acp-17-13001-2017,

719   2017.

720   Peng, L.Q., Zhang, Q., and He, K.B.: Emissions inventory of atmospheric pollutants

721   from open burning of crop residues in China based on a national questionnaire, Res.

722   Environ. Sci., 29, 1109-1118, 2016. (In Chinese)

723   Saxton, K.E., Kenny, J.F., and McCool, D.K.: Air permeability to define frozen soil

724   infiltration with variable tillage and residue, Trans. ASABE, 36, 1369-1375,

725   https://dx.doi.org/10.13031/2013.28472, 1993.

726   Schroeder, W., Oliva, P., Giglio, L., and Csiszar, I.A.: The New VIIRS 375 m active

727   fire detection data product: Algorithm description and initial assessment, Remote Sens.

728   Environ., 143, 85-96, https://dx.doi.org/10.1016/j.rse.2013.12.008, 2014.

729   Shi, W.J., Fang, Y.R., Chang, Y.Y., and Xie, G.H.: Toward sustainable utilization of crop

730   straw: Greenhouse gas emissions and their reduction potential from 1950 to 2021 in

731   China,   Resour.   Conserv.   Recy.,   190,   106824,

732   https://doi.org/10.1016/j.resconrec.2022.106824, 2023.

733   Song, Z.H., Zhang, L.M., Tian, C.G., Li, K.Y., Chen, P.Y., Jia, Z.Y., Hu, P., and Cui,

734   S.: Chemical characteristics, distribution patterns, and source apportionment of

735   particulate elements and inorganic ions in snowpack in Harbin, China, Chemosphere,

736   349, 140886, https://doi.org/10.1016/j.chemosphere.2023.140886, 2024.

737 Stavrakou, T., Müller, J.F., Bauwens, M., De Smedt, I., Lerot, C., Van Roozendael, M.,

738 Coheur, P.F., Clerbaux, C., Boersma, K.F. van der A, R., and Song, Y.: Substantial

739 underestimation of post-harvest burning emissions in the North China plain revealed

740 by multi-species space observations, Sci. Rep., 6, 32307,

741 https://dx.doi.org/10.1038/srep32307, 2016.

742 Stockwell, C.E., Yokelson, R.J., Kreidenweis, S.M., Robinson, A.L., DeMott, P.J.,

743 Sullivan, R.C., Reardon, J., Ryan, K.C., Griffith, D.W.T., and Stevens, L.: Trace gas

744 emissions from combustion of peat, crop residue, domestic biofuels, grasses, and other

745 fuels: configuration and Fourier transform infrared (FTIR) component of the fourth Fire

746 Lab at Missoula Experiment (FLAME-4), Atmos. Chem. Phys., 14, 9727-9754,

747 https://doi.org/10.5194/acp-14-9727-2014, 2014.

748 Sun, J.F., Peng, H.Y., Chen, J.M., Wang, X.M., Wei, M., Li, W.J., Yang, L.X., Zhang,

749 Q.Z., Wang, W.X., and Mellouki, A.: An estimation of CO_2 emission via agricultural

750 crop residue open field burning in China from 1996 to 2013, J. Clean. Prod., 112, 2625-

751 -2631, https://dx.doi.org/10.1016/j.jclepro.2015.09.112, 2016.

752 Syphard, A.D., Keeley, J.E., Pfaff, A.H., and Ferschweiler, K.: Human presence

753 diminishes the importance of climate in driving fire activity across the United States, P.

754 Natl. Acad. Sci. U.S.A., 114, 13750-13755, https://doi.org/10.1073/pnas.1713885114,

755 2017.

756 Tang, R., Huang, X., Zhou, D.R., and Ding, A.J.: Biomass-burning-induced surface

757 darkening and its impact on regional meteorology in eastern China, Atmos. Chem.

758   Phys., 20, 6177-6191, https://doi.org/10.5194/acp-20-6177-2020, 2020.

759   Tao, S., Ru, M.Y., Du, W., Zhu, X., Zhong, Q.R., Li, B.G., Shen, G.F., Pan, X.L., Meng,

760   W.J., Chen, Y.L., Shen, H.Z., Lin, N., Su, S., Zhuo, S.J., Huang, T.B., Xu, Y., Yun, X.,

761   Liu, J. F., Wang, X.L., Liu, W.X., Cheng, H.F., and Zhu, D.Q.: Quantifying the rural

762   residential energy transition in China from 1992 to 2012 through a representative

763   national survey, Nat. Energy, 3, 567-573, https://doi.org/10.1038/s41560-018-0158-4,

764   2018.

765   Tian, H., Zhao, D., and Wang, Y.: Emission inventories of atmospheric pollutants

766   discharged from biomass burning in China, Acta Sci. Circumstantiae, 31, 349-357, 2011.

767   (in Chinese)

768   Vadrevu, K., and Lasko, K.: Intercomparison of MODIS AQUA and VIIRS I-Band fires

769   and emissions in an agricultural landscape-implications for air pollution research,

770   Remote Sens., 10, 978, https://doi.org/10.3390/rs10070978, 2018.

771   van der Werf, G.R., Randerson, J.T., Giglio, L., van Leeuwen, T.T., Chen, Y., Rogers,

772   B.M., Mu, M.Q., van Marle, M.J.E., Morton, D.C., Collatz, G.J., Yokelson, R.J., and

773   Kasibhatla, P.S.: Global fire emissions estimates during 1997-2016, Earth Syst. Sci.

774   Data, 9, 697-720, https://doi.org/10.5194/essd-9-697-2017, 2017.

775   Vermote, E., Ellicott, E., Dubovik, O., Lapyonok, T., Chin, M., Giglio, L., and Roberts,

776   G.J.: An approach to estimate global biomass burning emissions of organic and black

777   carbon from MODIS fire radiative power, J. Geophys. Res., 114, D18

778   https://doi.org/10.1029/2008jd011188, 2009.

779   Wang, J.Y., Xi, F.M., Liu, Z., Bing, L.F., Alsaedi, A., Hayat, T., Ahmad., and Guan,

780   D.D.: The spatiotemporal features of greenhouse gases emissions from biomass burning

781   in China from 2000 to 2012, J. Clean. Prod., 181, 801-808,

782   https://doi.org/10.1016/j.jclepro.2018.01.206, 2018.

783   Wang, X.Y., Xue, S., and Xie, G.H.: Value-taking for residue factor as a parameter to

784   assess the field residue of field crops, J. China Agr. Univ., 17.1, 1-8, 2012. (in Chinese)

785   Weldemichael, Y., and Assefa, G.: Assessing the energy production and GHG

786   (greenhouse gas) emissions mitigation potential of biomass resources for Alberta, J.

787   Clean. Prod., 112, 4257-4264, https://doi.org/10.1016/j.jclepro.2015.08.118, 2016.

788   Wen, X., Chen, W.W., Chen, B., Yang, C.J., Tu, G., and Cheng, T.H.: Does the

789   prohibition on open burning of straw mitigate air pollution? An empirical study in Jilin

790   Province of China in the post-harvest season, J. Environ. Manage., 264, 110451,

791   https://doi.org/10.1016/j.jenvman.2020.110451, 2020.

792   Wiedinmyer, C., Kimura, Y., McDonald-Buller, E.C., Emmons, L.K., Buchholz, R.R.,

793   Tang, W.F., Seto, K., Joseph, M.B., Barsanti, K.C., Carlton, A.G., and Yokelson, R.:

794   The Fire Inventory from NCAR version 2.5: an updated global fire emissions model for

795   climate and chemistry applications, Geosci. Model Dev., 16, 3873-3891,

796   https://doi.org/10.5194/gmd-16-3873-2023, 2023.

797   Wiedinmyer, C., Yokelson, R.J., and Gullett, B.K.: Global emissions of trace gases,

798   particulate matter, and hazardous air pollutants from open burning of domestic waste,

799   Environ. Sci. Technol., 48, 16, 9523-9530, https://doi.org/10.1021/es502250z, 2014.

Wooster, M.J., Roberts, G., Perry, G.L.W., and Kaufman, Y.J.: Retrieval of biomass combustion rates and totals from fire radiative power observations: FRP derivation and calibration relationships between biomass consumption and fire radiative energy release, J. Geophys. Res-Atmos., 110, D24311, https://doi.org/10.1029/2005JD006318, 2005.

Wu, B.B., Li, J.H., Yao, Z.L., Li, X., Wang, W.J., Wu, Z.C., and Zhou, Q.: Characteristics and reduction assessment of GHG emissions from crop residue open burning in China under the targets of carbon peak and carbon neutrality, Sci. Total Environ., 905, 167235, https://doi.org/10.1016/j.scitotenv.2023.167235, 2023.

Wu, J., Kong, S.F., Wu, F.Q., Cheng, Y., Zheng, S.R., Qin, S., Liu, X., Yan, Q., Zheng, H., Zheng, M.M., Yan, Y.Y., Liu, D.T., Ding, S., Zhao, D.L., Shen, G.F., Zhao, T.L., and Qi, S.H.: The moving of high emission for biomass burning in China: View from multi-year emission estimation and human-driven forces. Environ. Int., 142, 105812, https://doi.org/10.1016/j.envint.2020.105812, 2020.

Wu, J., Kong, S.F., Wu, F.Q., Cheng, Y., Zheng, S.R., Yan, Q., Zheng, H., Yang, G.W., Zheng, M.M., Liu, D.T., Zhao, D.L., and Qi, S.H.: Estimating the open biomass burning emissions in central and eastern China from 2003 to 2015 based on satellite observation, Atmos. Chem. Phys., 18, 11623-11646, https://doi.org/10.5194/acp-18-11623-2018, 2018.

Xu, R.B., Ye, T.T., Yue, X., Yang, Z.Y., Yu, W.H., Zhang, Y.W., Bell, M.L., Morawska, L., Yu, P., Zhang, Y.X., Wu, Y., Liu, Y.M., Johnston, F., Lei, Y.D., Abramson, M.J., Guo,

821 Y.M., and Li, S.S.: Global population exposure to landscape fire air pollution from 2000

822 to 2019, Nature, 621, 521-529, https://doi.org/10.1038/s41586-023-06398-6, 2023a.

823 Xu, C., and You, C.: Agricultural expansion dominates rapid increases in cropland fires

824 in Asia, Environ. Int., 179, https://doi.org/108189, 10.1016/j.envint.2023.108189,

825 2023b.

826 Xu, W.D., Wooster, M.J., Kaneko, T., He, J.P., Zhang, T.R., and Fisher, D.: Major

827 advances in geostationary fire radiative power (FRP) retrieval over Asia and Australia

828 stemming from use of Himarawi-8 AHI, Remote Sens. Environ., 193, 138-149,

829 https://dx.doi.org/10.1016/j.rse.2017.02.024, 2017.

830 Xuan, F., Dong, Y., Li, J.Y., Li, X.C., Su, W., Huang, X.D., Huang, J.X., Xie, Z.X., Li,

831 Z.Q., Liu, H., Tao, W.C., Wen, Y.A., and Zhang, Y.: Mapping crop type in Northeast

832 China during 2013-2021 using automatic sampling and tile-based image classification,

833 Int. J. Appl. Earth Obs., 117, 103178, https://doi.org/10.1016/j.jag.2022.103178, 2023.

834 Yang, G.Y., Zhao, H.M., Tong, D.Q., Xiu, A.J., Zhang, X.L., and Gao, C.: Impacts of

835 post-harvest open biomass burning and burning ban policy on severe haze in the

836 Northeastern China, Sci. Total Environ., 716, 136517,

837 https://doi.org/10.1016/j.scitotenv.2020.136517, 2020.

838 Yang, Y., and Zhao, Y.: Quantification and evaluation of atmospheric pollutant

839 emissions from open biomass burning with multiple methods: a case study for the

840 Yangtze River Delta region, China, Atmos. Chem. Phys., 19, 327-348,

841 https://doi.org/10.5194/acp-19-327-2019, 2019.

Ying, L.X., Shen, Z.H., Yang, M.Z., and Piao, S.L.: Wildfire detection probability of modis fire products under the constraint of environmental factors: A study based on confirmed ground wildfire records, Remote Sens., 11, 24, 3031, https://doi.org/10.3390/rs11243031, 2019.

Zhang, X.H., Lu, Y., Wang, Q.G., and Qian, X.: A high-resolution inventory of air pollutant emissions from crop residue burning in China, Atmos. Environ., 213, 207-214, https://doi.org/10.1016/j.atmosenv.2019.06.009, 2019.

Zhang, T.R., de Jong, M.C., Wooster, M.J., Xu, W.D., and Wang, L.L.: Trends in eastern China agricultural fire emissions derived from a combination of geostationary (Himawari) and polar (VIIRS) orbiter fire radiative power products, Atmos. Chem. Phys., 20, 10687-10705, https://doi.org/10.5194/acp-20-10687-2020, 2020.

Zhao, H.M., Yang, G.Y., Tong, D.Q., Zhang, X.L., Xiu, A.J., and Zhang, S.C.: Interannual and seasonal variability of greenhouse gases and aerosol emissions from biomass burning in Northeastern China constrained by satellite observations, Remote Sens., 13, 1005, https://doi.org/10.3390/rs13051005, 2021.

Zheng, B., Ciais, P., Chevallier, F., Yang, H., Canadell, J.G., Chen, Y., van der Velde, I.R., Aben, I., Chuvieco, E., Davis, S.J., Deeter, M., Hong, C.P., Kong, Y.W., Li, H.Y., Li, H., Lin, X., He, K.B., and Zhang, Q.: Record-high CO_2 emissions from boreal fires in 2021, Science, 379, 912-917, https://doi.org/10.1126/science.ade0805, 2023.

Zhou, Y., Xia, X.C., Lang, J.L., Zhao, B.B., Chen, D.S., Mao, S.S., Zhang, Y.Y., Liu, J., and Li, J.: A coupled framework for estimating pollutant emissions from open burning

863 of specific crop residue: A case study for wheat, Sci. Total Environ., 844, 156731,

864 https://doi.org/10.1016/j.scitotenv.2022.156731, 2022.

865 Zhou, Y., Xing, X.F., Lang, J.L., Chen, D.S., Cheng, S.Y., Wei, L., Wei, X., and Liu, C.:

866 A comprehensive biomass burning emission inventory with high spatial and temporal

867 resolution in China, Atmos. Chem. Phys., 17, 2839-2864, https://doi.org/10.5194/acp-

868 17-2839-2017, 2017.

869 Zhuang, Y., Li, R.Y., Yang, H., Chen, D.L., Chen, Z.Y., Gao, B.B., and He, B.:

870 Understanding temporal and spatial distribution of crop residue burning in China from

871 2003 to 2017 using MODIS data, Remote Sens., 10(3), 390,

872 https://doi.org/10.3390/rs10030390, 2018.

873 Zhu, C., Kawamura, K., and Kunwar, B.: Effect of biomass burning over the western

874 North Pacific Rim: Wintertime maxima of anhydrosugars in ambient aerosols from

875 Okinawa, Atmos. Chem. Phys., 15, 1959-1973, https://doi.org/10.5194/acp-15-1959-

876 2015, 2015.